

# Preparation of CO<sub>2</sub> adsorbent with N<sup>1</sup>-(3-(trimethoxysilyl)propyl)-1,3-propanediamine and its performance

Tristan James Sim, Rose Mardie Pacia, and Young Soo Ko<sup>†</sup>

Department of Chemical Engineering, Kongju National University, 1223-24 Cheonan-daero, Seobuk-gu, Cheonan 31080, Korea

(Received 9 February 2020 • Revised 9 April 2020 • Accepted 30 April 2020)

**Abstract**—N<sup>1</sup>-(3-(trimethoxysilyl)propyl)-1,3-propanediamine (2NS-P), a diaminosilane having a propyl spacer between the two amino groups was successfully synthesized, and a CO<sub>2</sub> adsorbent functionalized with 2NS-P was prepared via impregnation of it into silica. The adsorption performance and stability of 2NS-P/Kona95 were examined and compared to that of N<sup>1</sup>-(3-(trimethoxysilyl)propyl)ethane-1,2-diamine (2NS)/Kona95 having an ethyl spacer. 2NS-P/Kona95 exhibited better CO<sub>2</sub> adsorption capacity and CO<sub>2</sub>/N efficiency. The adsorbents were subjected to ten cycles of temperature swing adsorption (TSA), demonstrating that stability of 2NS-P/Kona95 was better than that of 2NS/Kona95. The spent 2NS-P/Kona95 showed the absence of cyclic urea formation in FT-IR spectrum, explaining the better stability of 2NS-P/Kona95 than 2NS/Kona95.

Keywords: CO<sub>2</sub> Adsorption, Amine Structure, Adsorbent, Temperature Swing Adsorption

## INTRODUCTION

Carbon dioxide (CO<sub>2</sub>) emission has been the primary source of increasing greenhouse gas concentration in the atmosphere. The most consistently researched and applied technology of CO<sub>2</sub> capture is post-combustion capture (PCC) [1-3]. CO<sub>2</sub> absorption with aqueous amine solutions has become a promising technology [4], but this process is flawed with several problems [5] such as volatile amine loss and high energy utilization for regeneration, among others [1,6,7]. To overcome such drawbacks, solid adsorbents (e.g., organic/inorganic hybrid) for dry CO<sub>2</sub> capture have been developed as potential substitutes due to their capability of reversibly capturing CO<sub>2</sub>, increased CO<sub>2</sub> capture capacity, and greater selectivity [7].

Among a diversity of solid adsorbents, those functionalized with amines are preferred owing to their high CO<sub>2</sub> adsorption selectivity in a real flue gas condition [8-10]. Such materials can be fabricated by the heterogenization of amines in porous supports via impregnation, grafting, or polymerization of amine monomers within the pores [11-14]. In addition, their facile regeneration, increased adsorption capacity, and fast adsorption kinetics make amine-containing supports more desirable for CO<sub>2</sub> capture [9,15].

Amines for CO<sub>2</sub> adsorbents are categorized by the number of the amine's alkyl groups and on the number of nitrogen atoms. The properties and performance of the adsorbents depend on the type of amine incorporated [16]. In actual operation, the key factors in considering functionalized CO<sub>2</sub> adsorbents are their recyclability and stability. Consequently, the adsorbent must be resistant to degradation at high temperature to ensure its efficiency in the long run.

One of the intensively studied amine-containing adsorbents was functionalized by N<sup>1</sup>-(3-(trimethoxysilyl)propyl)ethane-1,2-diamine

(2NS). Diamines were expected to demonstrate a higher capacity due to their higher nitrogen content than monoamines. The present challenge, however, in employing these kinds of diamine-functionalized adsorbents is that they tend to form irreversible degradation species which lowers their adsorption capacity. At high temperature, primary amines react with CO<sub>2</sub> to form cyclic urea as with monoamines, while secondary amines react with O<sub>2</sub> to form amides [14,17-19]. Research endeavors on diamines and polyamines with an ethyl spacer (N atoms separated by 2 carbons) have dominated CO<sub>2</sub> capture technology in recent years [20-22]. However, little attention has been devoted in elucidating the characteristics and performance of diamines with a propyl spacer [23,24].

In this study, we first synthesized N<sup>1</sup>-(3-(trimethoxysilyl)propyl)-1,3-propanediamine (2NS-P), a diaminosilane having a propyl spacer between its two amine groups, and subsequently immobilized it onto silica to prepare the functionalized CO<sub>2</sub> adsorbent. Characterization of 2NS-P was via <sup>1</sup>H-NMR. Physical properties of the CO<sub>2</sub> adsorbent were further examined and compared with that of an adsorbent containing 2NS. We also investigated and compared the cyclic stabilities of the prepared adsorbents by thermal gravimetric analysis and TSA simulation to assess CO<sub>2</sub> adsorption stability.

## EXPERIMENTAL

### 1. Materials

To prepare Kona95, a mixture composed of 0.95 kg fumed (pyrogenic) silica (KONASIL K-300, OCI), 0.05 kg silica sol (Ludox AS-30, Aldrich), and 9 kg water was first produced. The resulting slurry was spray-dried in order to afford the silica, Kona95 which was subsequently calcined at 600 °C in dry air. N<sup>1</sup>-(3-(trimethoxysilyl)propyl)ethane-1,2-diamine (2NS, 97%, Alfa Aesar) is the diaminosilane containing an ethyl spacer. In addition, the reactants for the synthesis of (2NS-P) were 3-(chloropropyl)-trimethoxysilane (CPTMS, 97%, Aldrich) and 1,3-propanediamine (DAP, 98%, Aldrich). CPTMS

<sup>†</sup>To whom correspondence should be addressed.

E-mail: ysko@kongju.ac.kr

Copyright by The Korean Institute of Chemical Engineers.

and DAP were transferred and stored in bottles under nitrogen atmosphere.  $\text{CDCl}_3$  (99.8 atom% D, Aldrich) used as solvent for  $^1\text{H}$  NMR analysis were used without further purification. Ultra-high purity gases, nitrogen (99.999%) and  $\text{CO}_2$  purchased from Daeduk Gas. Molecular sieve 5A/13X and Fisher RIDOX columns were used to further purify the nitrogen gas.

## 2. Synthesis of $\text{N}^1$ -(3-(trimethoxysilyl)propyl)-1,3-propanediamine (2NS-P)

Prior to the reaction, a round-bottom flask was evacuated, then purged with  $\text{N}_2$  in a Schlenk line. 5.5 mL of CPTMS was injected into the flask, followed by dropwise addition of 5.0 mL of DAP at room temperature. The reaction was then allowed to proceed at  $80^\circ\text{C}$  for 12 h with stirring. The product was separated via syringe filtration. The recovered liquid was transferred and sealed in a vial containing nitrogen gas. The proposed reaction mechanism is illustrated in Fig. 1.

## 3. Preparation of Adsorbent

A separate flask carrying 1.0 g Kona95 was also subjected to nitrogen atmosphere. Then, 6 mmol diaminosilane was added to Kona95 dropwise with gentle stirring. The temperature was then elevated to  $50^\circ\text{C}$  and the mixture was allowed to react for 3 h. 2NS/Kona95 and 2NS-P/Kona95 were the corresponding designations for the synthesized adsorbents.

## 4. Characterization and $\text{CO}_2$ Capture Performance

To confirm the structure of the synthesized 2NS-P,  $^1\text{H}$  NMR

analysis was carried out on Bruker AVANCE III 400.  $\text{CDCl}_3$  was used as solvent and all spectra were analyzed at room temperature. FT-IR analyses were conducted in a Thermo Scientific NICOLET 6700 Spectrometer. 0.1-1.0% of a sample was mixed with 200 mg KBr and then formed into discs for FT-IR analysis. Degassing of the samples at  $110^\circ\text{C}$  under vacuum conditions for 1 h was performed before IR spectra collection. Upon cooling of the system to room temperature, IR spectra were recorded with 32 scans at a resolution of  $4\text{ cm}^{-1}$ .

Physical properties of the support and the adsorbents were measured by  $\text{N}_2$  adsorption/desorption isotherms (ASAP 2020, Micromeritics) at  $-196^\circ\text{C}$ . The samples were first degassed at  $110^\circ\text{C}$  and 670  $\mu\text{bar}$  overnight to remove pre-adsorbed species. The BET surface area ( $S_{\text{BET}}$ ) was calculated over a relative pressure range ( $P/P_0$ ) of 0.05-0.20 and the total pore volume at  $P/P_0=0.99$ . A Flash 2000 Organic Elemental Analyzer was used to obtain the adsorbents' nitrogen contents. These %N values were then used to calculate the silane contents using Eq. (1).

$$\begin{aligned} \text{silane content (mmol/g)} &= \frac{\% \text{N from elemental analysis}}{100} \\ &\times \frac{1 \text{ mol}}{14.01 \text{ g}} \times \frac{1000 \text{ mmol}}{1 \text{ mol}} \times \frac{1 \text{ mmol amine}}{\text{mmol N}} \end{aligned} \quad (1)$$

Fresh  $\text{CO}_2$  adsorption capacities were determined by exposing 50 mg of the adsorbents to a 60 mL/min of 17%  $\text{CO}_2$ /balance  $\text{N}_2$

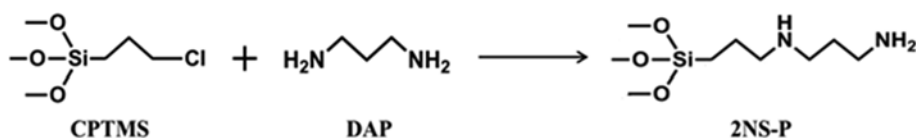


Fig. 1. Scheme of the synthesis of  $\text{N}^1$ -(3-(trimethoxysilyl)propyl)-1,3-propanediamine.

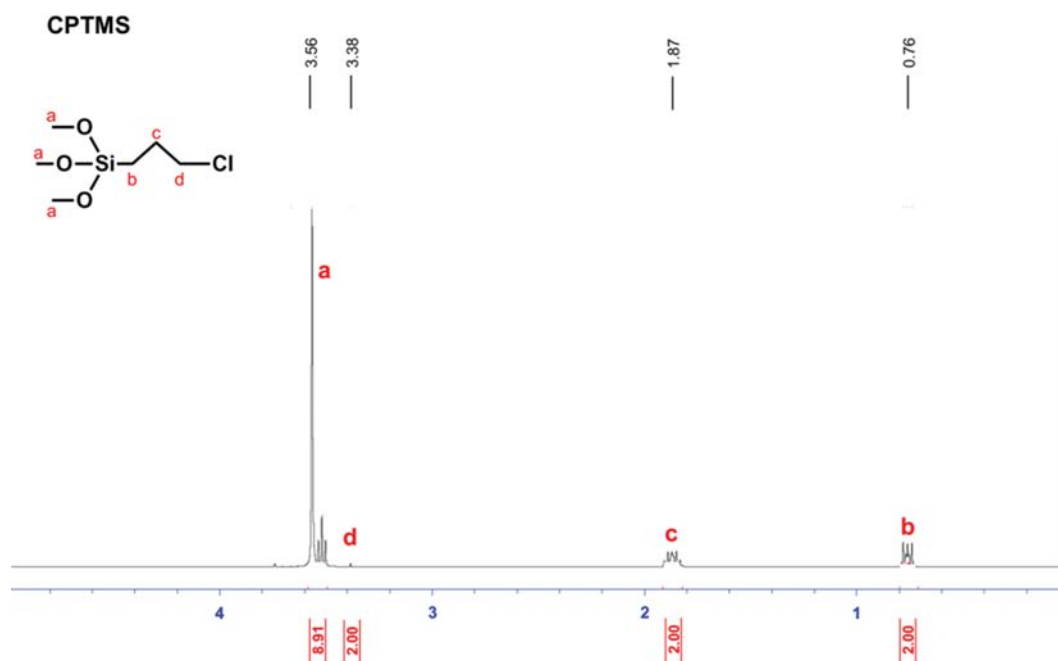


Fig. 2.  $^1\text{H}$ -NMR spectrum of CPTMS.

mixture gas for 1 h at 30 °C in a thermal gravimetric analyzer (TGA, SDT Q600, TA Instruments). Pretreatment of the adsorbents (degassing) with 60 mL/min of N<sub>2</sub> for 1 h at 110 °C in TG was done prior to the measurement of fresh CO<sub>2</sub> adsorption capacity. Thermal stability (24 h exposure to CO<sub>2</sub>) and TSA cyclic stability were also evaluated in TG. Pretreatment of the adsorbents (degassing) with 60 mL/min of N<sub>2</sub> for 1 h at 110 °C in TG was also done prior to thermal stability and cyclic stability tests. The selected temperature

for thermal stability test for 24 h was 110 °C at which CO<sub>2</sub> and amine react to form cyclic urea [14,23]. During the thermal stability test, 60 mL/min of 100% CO<sub>2</sub> gas was flowed into TG for 24 h. Then, the adsorbents were regenerated at the same temperature for 90 min under flowing N<sub>2</sub>. Meanwhile, cyclic stability was assessed by employing a simulated TSA process. After pretreatment, the adsorbents were subjected to adsorption by flowing 60 mL/min of 17% CO<sub>2</sub>/balance N<sub>2</sub> for 10 minutes at 30 °C [14]. Afterwards, the

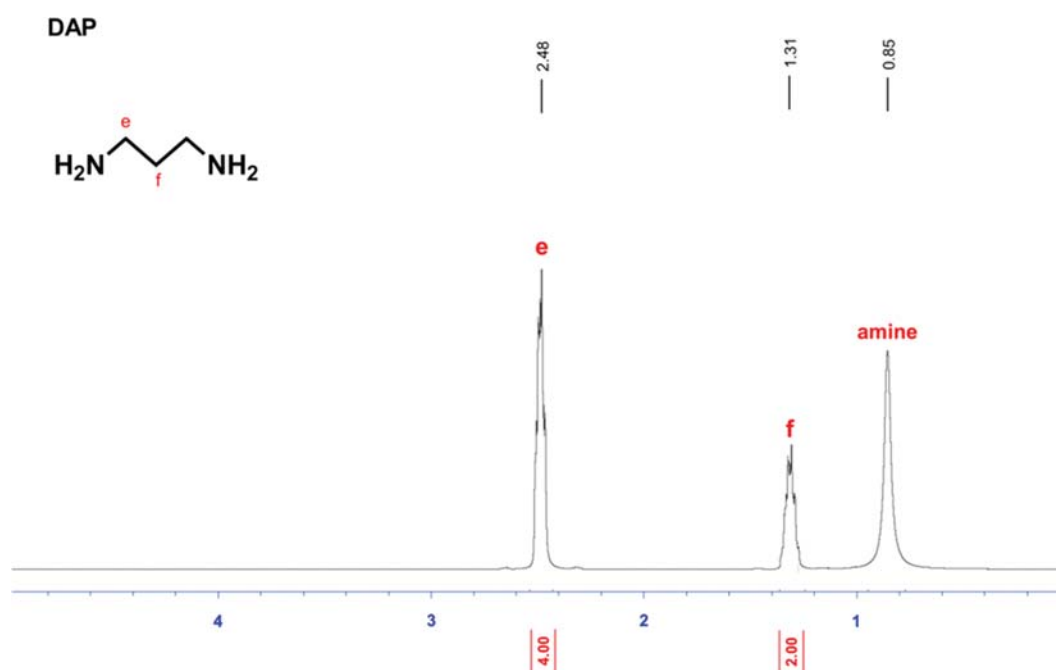


Fig. 3. <sup>1</sup>H-NMR spectrum of DAP.

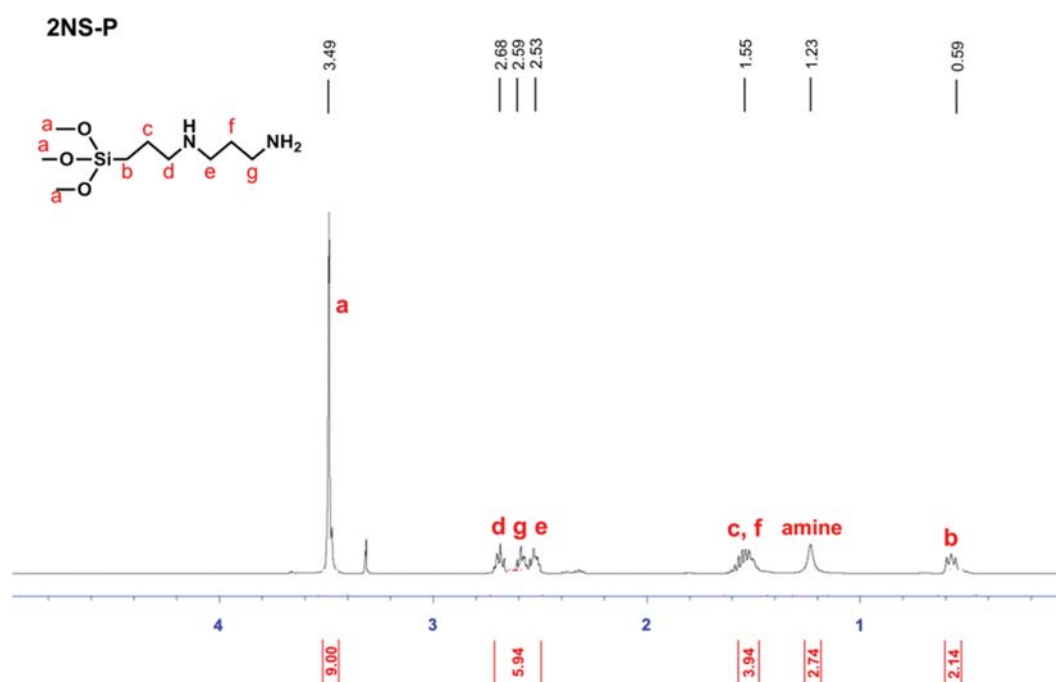


Fig. 4. <sup>1</sup>H-NMR spectrum of the synthesized 2NS-P.

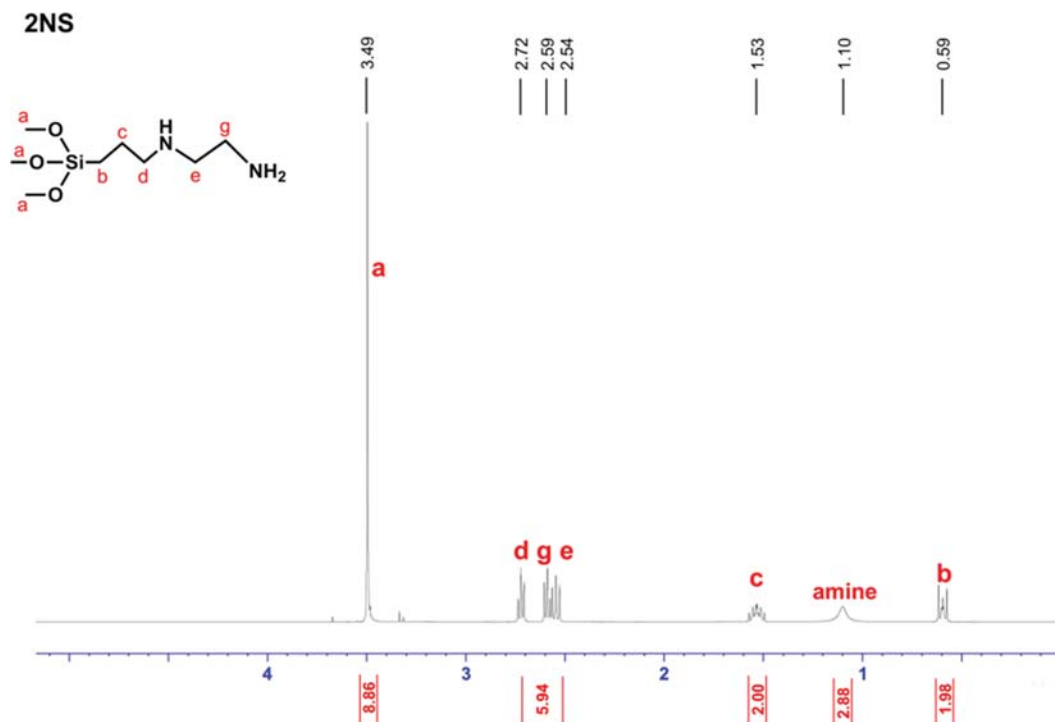


Fig. 5.  $^1\text{H-NMR}$  spectrum of 2NS.

flowing gas was switched to 100%  $\text{CO}_2$  while the temperature was ramped to  $110^\circ\text{C}$ . At this temperature,  $\text{CO}_2$  desorption took place for 10 min. Then, the adsorbents were cooled to  $30^\circ\text{C}$  with flowing  $\text{N}_2$  before starting another adsorption step. The adsorption-desorption process was repeated ten times.

## RESULTS AND DISCUSSION

### 1. Characterization of Synthesized 2NS-P

The synthesized diaminosilane with a propyl spacer (2NS-P) was characterized through  $^1\text{H-NMR}$  spectroscopy to establish the completion of the reaction. Figs. 2-5 depict, respectively,  $^1\text{H-NMR}$  spectra of CPTMS, DAP, 2NS-P, and 2NS. The peak corresponding to the methoxy group of 2NS-P was seen at 3.49 ppm. This peak was also observed from 2NS at 3.49 ppm. The propyl chain attached to Si of 2NS-P was observed at 0.59, 1.55, and 2.68 ppm. A considerable change was detected for the shift assigned to **d**. This confirms the successful substitution with DAP to Cl. In addition, peaks corresponding to the propyl spacer between two amines were detected at 1.55, 2.53, and 2.59 ppm. The presence of these chemical shifts was also found in 2NS except the peak assigned to **f**, which corresponds to the additional  $-\text{CH}_2$  group in 2NS-P. Therefore, under the conditions presented in this work, 2NS-P was successfully prepared.

### 2. Characterization of the Adsorbents

Along with the corresponding silane contents, Table 1 summarizes the physical properties of the silica support (Kona95) and the synthesized adsorbents. To make a direct evaluation and comparison, the adsorbents were prepared with similar silane loadings. Upon amine functionalization, both surface areas and total pore volumes reduced compared to the bare support.

Table 1. Physical properties of the silica and the synthesized adsorbents

Sample	Silane content (mmol/g)	$S_{\text{BET}}$ ( $\text{m}^2/\text{g}$ ) <sup>a</sup>	$V_p$ ( $\text{cm}^3/\text{g}$ ) <sup>b</sup>
Kona95	-	253	0.765
2NS/Kona95	3.19	18	0.105
2NS-P/Kona95	2.50	23	0.114

<sup>a</sup>Surface areas were calculated from BET at  $P/P_0=0.05-0.20$ .

<sup>b</sup>Total pore volumes were declared as the amount of adsorbed nitrogen at  $P/P_0=0.99$ .

Fig. 6 shows the TGA curves of the diaminosilanes, silica support, and adsorbents. The points of inflection of 2NS and 2NS-P were observed at  $145^\circ\text{C}$  and  $175^\circ\text{C}$ , respectively (Fig. 6(a)). These temperatures relate to the decomposition temperatures of the diaminosilanes. Kona95 exhibited a negligible mass loss and was found to be stable up to  $800^\circ\text{C}$ . Meanwhile, both adsorbents exhibited three mass losses (Fig. 6(b)). The first mass loss occurred at about  $100^\circ\text{C}$ , which corresponds to the evaporation of physisorbed water molecules [25]. The second mass loss was observed at  $150^\circ\text{C}$  and  $230^\circ\text{C}$  for 2NS/Kona95 and 2NS-P/Kona95, respectively, which were attributed to amine degradation [26,27]. Lastly, the decline from  $380^\circ\text{C}$  to  $800^\circ\text{C}$  was associated with the total decomposition of the alkoxy groups in the adsorbents.

FT-IR analyses revealed the spectral differences between the bare support and functionalized adsorbents as shown in Fig. 7. The bare Kona95 demonstrated a sharp peak at  $3,747\text{ cm}^{-1}$  which is ascribed to an Si-OH group. This peak's intensity was observed to notably

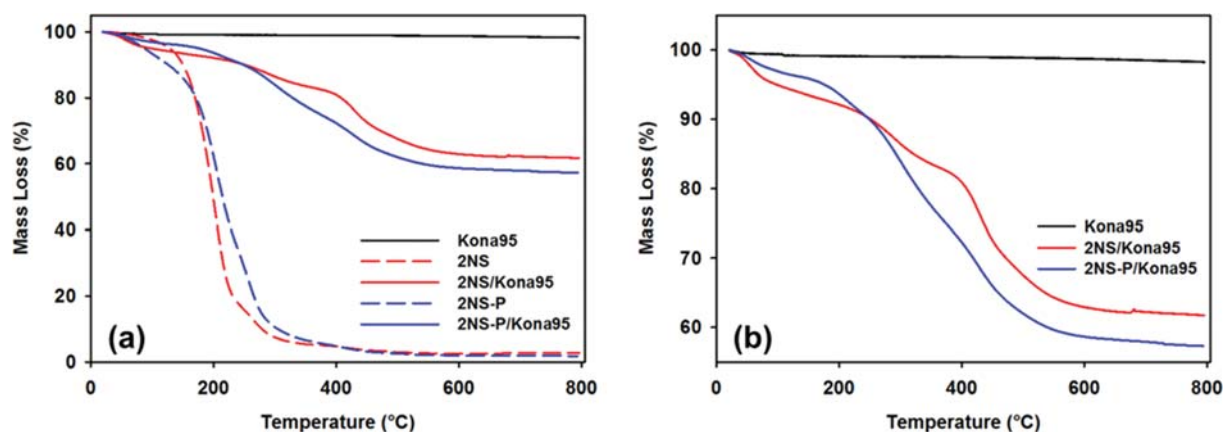


Fig. 6. TG curves of (a) Kona95-supported adsorbents and diaminosilanes, and (b) Kona95-supported adsorbents (enlarged).

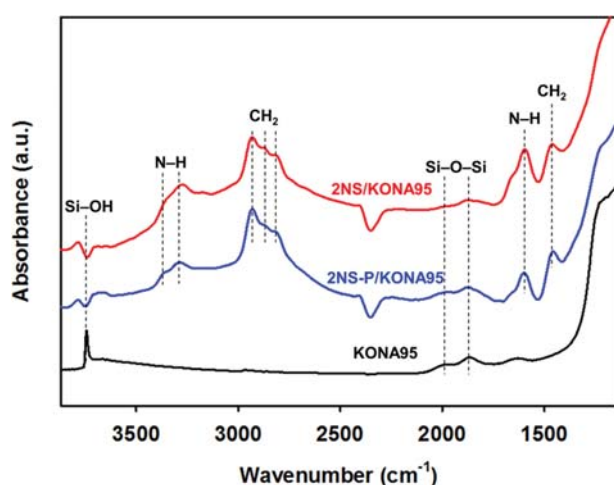


Fig. 7. FT-IR spectra of Kona95 and functionalized adsorbents.

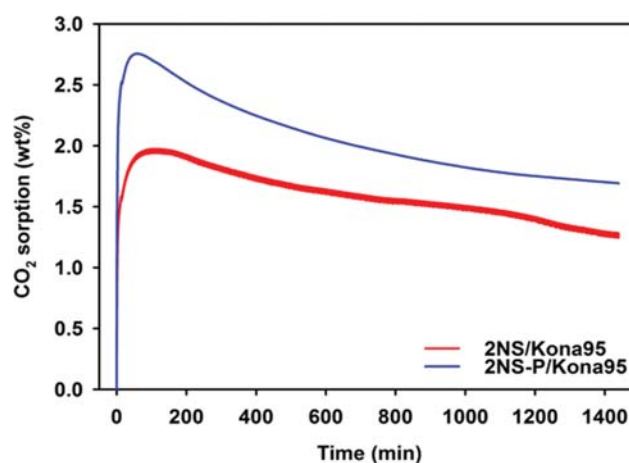


Fig. 8. Functionalized adsorbents' mass changes upon 24-h exposure to 100% CO<sub>2</sub> at 110 °C.

decrease with respect to the functionalized materials, which means that the silanol groups were involved in the functionalization with 2NS and 2NS-P. The successful functionalization was confirmed with the appearance of the functional groups of the diaminosilanes such as NH<sub>2</sub> and CH<sub>2</sub> peaks. N-H stretching and bending vibrations were also observed at 3,250-3,400 cm<sup>-1</sup> and at 1,580-1,650 cm<sup>-1</sup>, respectively. Moreover, C-H stretching, and vibrations were, respectively, found at 2,850-2,950 cm<sup>-1</sup> and 1,430-1,470 cm<sup>-1</sup>. The presence of the expected functional groups in 2NS-P-functionalized silica at the corresponding positions on the spectrum indicates the

successful anchorage of diaminosilanes onto the silica frameworks.

### 3. Stability of Adsorbents

As shown in Table 2, both fresh 2NS/Kona95 and 2NS-P/Kona95 showed a CO<sub>2</sub> adsorption capacity of 6.70 wt%. The CO<sub>2</sub> physical adsorption amount of pure silica (Kona95) was lower than 0.3 wt% at 30 °C. To assess the stability of adsorbents over long periods of time, both adsorbents were exposed to 100% CO<sub>2</sub> at 110 °C for 24 h in the TGA. After the 24-h exposure, the CO<sub>2</sub> adsorption capacity of 2NS/Kona95 and 2NS-P/Kona95 was reduced to 1.27 and 2.17 wt%, respectively. 2NS-P demonstrated a better stability

Table 2. Percentage decrease in CO<sub>2</sub> adsorption capacity upon 24-h exposure to 100% CO<sub>2</sub> at 110 °C in the TGA

Sorbents	Silane content (mmol/g) <sup>a</sup>	Fresh CO <sub>2</sub> sorption (wt%) <sup>b</sup>	Exposure at 110 °C	
			CO <sub>2</sub> sorption (wt%)	
			Spent	% Decrease
2NS/Kona95	3.19	6.70	1.27	81
2NS-P/Kona95	2.50	6.70	2.17	68

<sup>a</sup>Calculated using Eq. (1).

<sup>b</sup>Exposure conditions: 60 mL/min, 17% CO<sub>2</sub>/balance N<sub>2</sub>, 30 °C, 1 h.

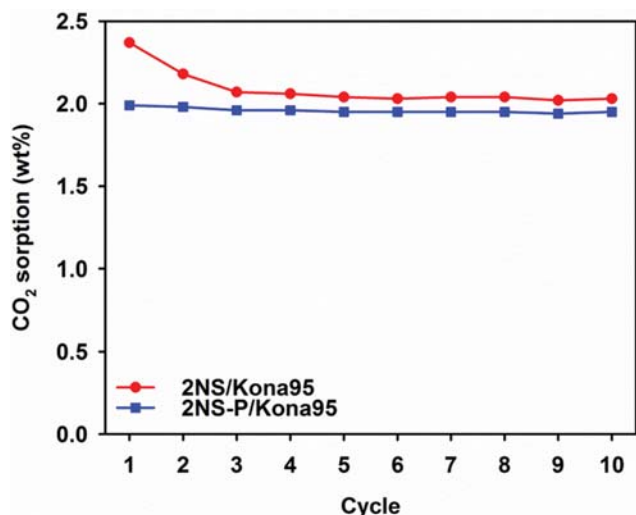


Fig. 9. CO<sub>2</sub> adsorption capacity for TSA cycles over 2NS/Kona95 and 2NS-P/Kona95 in CO<sub>2</sub> (17%) for 10 min at 30 °C.

than 2NS though CO<sub>2</sub> adsorption capacity of both adsorbents decreased dramatically. Fig. 8 reveals the mass changes in adsorbents for the entire 24-h run at 110 °C in the TGA. The change in mass of adsorbent during the 24-h exposure corresponds to the change in CO<sub>2</sub> adsorption. At an exposure temperature of 110 °C, 2NS-P/Kona95 showed a greater CO<sub>2</sub> uptake than 2NS/Kona95 though the former had a lower silane content. This means that 2NS-P/Kona95 possesses a higher CO<sub>2</sub>/N efficiency than its counterpart. The higher CO<sub>2</sub> adsorption capacity and CO<sub>2</sub>/N efficiency of 2NS-P/Kona95 could be attributed to the stronger basicity (pK<sub>a</sub>) of amine and weakening of interaction with the next amine due to the longer alkyl spacer [28,29]. The final CO<sub>2</sub> uptakes for 2NS/Kona95 and 2NS-P/Kona95 after 24 h were 1.26 wt% and 1.69 wt%, respectively.

CO<sub>2</sub> adsorbents for TSA processes should be recycled more than a few thousand times. To compare and evaluate the cyclic performance of the adsorbents, ten adsorption-desorption cyclic experiments were employed in the TGA. Fig. 9 presents the TSA results for both adsorbents in an environment of CO<sub>2</sub> (17%). The first CO<sub>2</sub> adsorption capacity in the cyclic experiments (<3 wt%) was lower than that of the fresh CO<sub>2</sub> adsorption (>6 wt%), resulting from difference in adsorption time. It was demonstrated that 2NS-P/Kona95 was stable up to ten cycles, which only underwent a capacity decrease of 2.0% compared to the 14.4% decrease of 2NS/Kona95. The fresh and spent adsorbents after ten cyclic experiments were analyzed with FT-IR to investigate the differences in degradation species as shown in Fig. 10. The spent 2NS/Kona95 exhibited mainly the formation of cyclic urea [14,18]. Meanwhile, no cyclic urea was found in the spent 2NS-P/Kona95, but only small peaks of carbamic acid and silylpropylcarbamate were present. In addition, peaks of carbamate ion (symmetric stretching, 1,430 cm<sup>-1</sup> and asymmetric stretching, 1,565-1,555 cm<sup>-1</sup>) and -NH<sub>3</sub><sup>+</sup> ion (symmetric deformation, 1,490-1,480 cm<sup>-1</sup> and asymmetric deformation, 1,640-1,630 cm<sup>-1</sup>) have also been observed from the spectra [30]. The reaction between amine and CO<sub>2</sub> had been generally reported to generate three species: carbamate, carbamic acid, and silylpropylcarbamate [31]. These species can be converted again to amine with CO<sub>2</sub> gen-

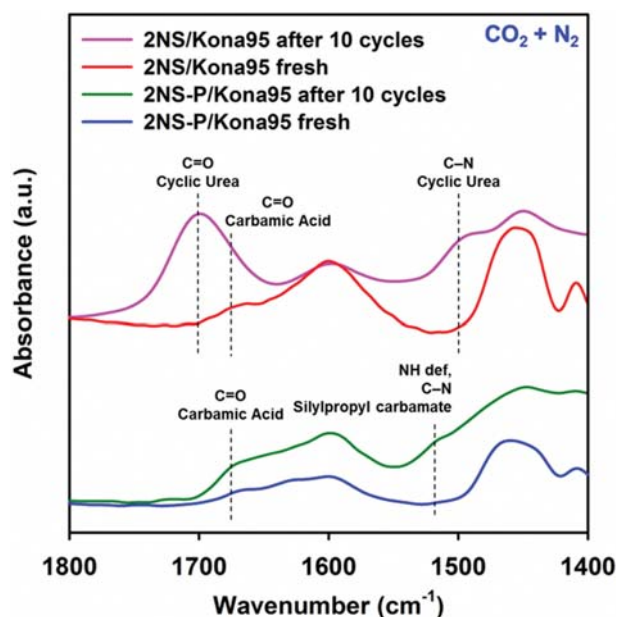


Fig. 10. FT-IR spectra of 2NS/Kona95 and 2NS-P/Kona95 before (fresh) and after (spent) 10 TSA cycles in CO<sub>2</sub> (17%).

eration at a higher temperature, but each species has its own corresponding desorption temperature [16]. Nonetheless, even ten cyclic experiments for 2NS/Kona95 caused the formation of cyclic urea, which was reported to be an irreversible product of degraded CO<sub>2</sub> amine adsorbent [19]. Therefore, the better stability of 2NS-P/Kona95 can be explained by no formation of cyclic urea. The better stability of 2NS-P can also result from the secondary amine with propyl spacer.

## CONCLUSIONS

2NS-P, a diaminosilane containing a propyl spacer that bridges two of its amine groups, was successfully synthesized and confirmed by <sup>1</sup>H-NMR. The 2NS and 2NS-P were then impregnated (by incipient wetness) to silica, Kona95. Both functionalized adsorbents demonstrated comparable adsorption performance, with 2NS-P/Kona95 showing a better one in terms of increased CO<sub>2</sub> sorption capacity and thermal cyclic stability. The alkyl spacer brings a considerable positive effect to the functionalized adsorbent's CO<sub>2</sub> adsorption properties.

## ACKNOWLEDGEMENTS

This work was supported by a National Research Foundation of Korea (NRF) grant funded by the government of Korea (MSIP) (2016R1D1A1B01009941). Financial grants for this endeavor were also provided by the Human Resources Program in Energy Technology of the Korea Institute of Energy Technology Evaluation and Planning (KETEP) under the Ministry of Trade, Industry & Energy, Republic of Korea (No. 20194010201730).

## REFERENCES

1. J. Oexmann and A. Kather, *Int. J. Greenh. Gas Control*, **4**, 36 (2010).

2. I. Kim and H. F. Svendsen, *Ind. Eng. Chem. Res.*, **46**, 5803 (2007).
3. B. P. Spigarelli and S. K. Kawatra, *J. CO<sub>2</sub> Util.*, **1**, 69 (2013).
4. G. T. Rochelle, *Science*, **325**, 1652 (2009).
5. D. M. D'Alessandro, B. Smit and J. R. Long, *Angew. Chem. Int. Ed.*, **49**(35), 6058 (2010).
6. I. Sreedhar, T. Nahar, A. Venugopal and B. Srinivas, *Renew. Sustain. Energy Rev.*, **76**, 1080 (2017).
7. A. Samanta, A. Zhao, G. K. H. Shimizu, P. Sarkar and R. Gupta, *Ind. Eng. Chem. Res.*, **51**(4), 1438 (2012).
8. R. V. Siriwardane, M. Shen, E. P. Fisher and J. A. Poston, *Energy Fuels*, **15**(2), 279 (2001).
9. S. Choi, J. H. Drese and C. W. Jones, *ChemSusChem*, **2**, 796 (2009).
10. J. Wang, L. Huang, R. Yang, Z. Zhang, J. Wu, Y. Gao, Q. Wang, D. O'Hare and Z. Zhong, *Energy Environ. Sci.*, **7**, 3478 (2014).
11. K. Min, W. Choi, C. Kim, C. Kim and M. Choi, *Nat. Commun.*, **9**, 726 (2018).
12. D. H. Kim, J. Celedonio and Y. S. Ko, *Top. Catal.*, **60**, 706 (2017).
13. D. H. Kim and Y. S. Ko, *Res. Chem. Intermed.*, **44**, 3661 (2018).
14. C. Maniangu, R. M. Pacia and Y. S. Ko, *Korean J. Chem. Eng.*, **36**(8), 1267 (2019).
15. P. Bollini, S. A. Didas and C. W. Jones, *J. Mater. Chem.*, **21**(39), 15100 (2011).
16. J. H. Park, J. M. Celedonio, H. Seo, Y. K. Park and Y. S. Ko, *Catal. Today*, **265**, 68 (2016).
17. A. Sayari, A. Heydari-Gorji and Y. Yang, *J. Am. Chem. Soc.*, **134**(33), 13834 (2012).
18. A. Heydari-Gorji and A. Sayari, *Ind. Eng. Chem. Res.*, **51**(19), 6887 (2012).
19. J. M. Celedonio, R. M. Pacia and Y. S. Ko, *Catal. Today*, **303**, 55 (2018).
20. A. F. Ciftja, A. Hartono and H. F. Svendsen, *Energy Procedia*, **37**, 1605 (2013).
21. M. J. O'Brien, R. L. Farnum and R. J. Perry, *Energy Fuels*, **27**(1), 467 (2013).
22. W. Choi, K. Min, C. Kim, Y. S. Ko, J. W. Jeon, H. Seo, Y.-K. Park and M. Choi, *Nat. Commun.*, **7**, 12640 (2016).
23. S. H. Pang, L. C. Lee, M. A. Sakwa-Novak, R. P. Lively and C. W. Jones, *J. Am. Chem. Soc.*, **139**(10), 3627 (2017).
24. R. M. Pacia, C. Maniangu and Y. S. Ko, *Catalysts*, **9**(11), 910 (2019).
25. S. Cerveny, G. A. Schwartz, J. Otegui, J. Colmenero, J. Loichen and S. Westermann, *J. Phys. Chem. C*, **116**(45), 24340 (2012).
26. K. Li, J. Jang, F. Yan, S. Tian and X. Chen, *Appl. Energy*, **136**, 750 (2014).
27. K. M. Hello, A. A. Ibrahim, J. K. Shneine and J. N. Appaturi, *South African J. Chem. Eng.*, **25**, 159 (2018).
28. M. Borkovec and G. J. M. Koper, *J. Phys. Chem.*, **98**(23), 6038 (1994).
29. G. J. M. Koper, M. H. P. Van Genderen, C. Elissen-Román, M. W. P. L. Baars, E. W. Meijer and M. Borkovec, *J. Am. Chem. Soc.*, **119**(28), 6512 (1997).
30. N. Hedin and Z. Bacsik, *Curr. Opin. Green Sustain. Chem.*, **16**, 13 (2019).
31. C. H. Chen, D. Shimon, J. J. Lee, S. A. Didas, A. K. Mehta, C. Sievers, C. W. Jones and S. E. Hayes, *Environ. Sci. Technol.*, **51**, 6553 (2017).